Improving MR Image Quality in Patients with Metallic Implants

Elizabeth M. Lee, MD
El-Sayed H. Ibrahim, PhD
Nancy Dudek, BS
Jimmy C. Lu, MD
Vivek Kalia, MD, MPH, MS
Mason Runge, MD
Ashok Srinivasan, MBBS
Jadranka Stojanovska, MD, MS
Prachi P. Agarwal, MBBS, MS

The number of implanted devices such as orthopedic hardware and cardiac implantable devices continues to increase with an increase in the age of the patient population, as well as an increase in the number of indications for specific devices. Many patients with these devices have or will develop clinical conditions that are best depicted at MRI. However, implanted devices containing paramagnetic or ferromagnetic substances can cause significant artifact, which could limit the diagnostic capability of this modality. Performing imaging with MRI when an implant is present may be challenging, and there are numerous techniques the radiologist and technologist can use to help minimize artifacts related to implants. First, knowledge of the presence of an implant before patient arrival is critical to ensure safety of the patient when the device is subjected to a strong magnetic field. Once safety is ensured, the examination should be performed with the MRI system that is expected to provide the best image quality. The selection of the MRI system includes multiple considerations such as the effects of field strength and availability of specific sequences, which can reduce metal artifact. Appropriate patient positioning, attention to MRI parameters (including bandwidth, voxel size, and echo), and appropriate selection of sequences (those with less metal artifact and advanced metal reduction sequences) are critical to improve image quality. Patients with implants can be successfully imaged with MRI with appropriate planning and understanding of how to minimize artifacts. This improves image quality and the diagnostic confidence of the radiologist.

Abbreviations: CIED = cardiac implantable electronic device, FSE = fast spin echo, LGE = late gadolinium enhancement, MARS = metal artifact reduction sequence, MAVRIC = multiacquisition with variable-resonance image combination, SAR = specific absorption rate, SEMAC = slice encoding for metal artifact correction, SNR = signal-to-noise ratio, SPIR = spectral presaturation with inversion recovery, SSFP = steady-state free precession, STIR = short τ inversion recovery, TE = echo time, TR = repetition time

RadioGraphics 2021; 41:0000–0000

https://doi.org/10.1148/rg.2021200092

Content Codes: CA MR PH SQ

From the Department of Radiology, Division of Cardiothoracic Imaging (E.M.L., J.S., P.P.A.), Department of Radiology (N.D.), Department of Pediatrics, Division of Cardiology, CS Mott Children's Hospital (J.C.L.), Department of Radiology, Division of Musculoskeletal Radiology (V.K.), University of Michigan Medical School (M.R.), and Department of Radiology, Division of Neuroradiology (A.S.), University of Michigan, University Hospital Floor B1 Reception C, 1500 E Medical Center Dr, SPC 5030, Ann Arbor, MI 48109; and Center for Imaging Research, Medical College of Wisconsin, Milwaukee, Wis (E.H.I.). Presented as an education exhibit at the 2019 RSNA Annual Meeting. Received April 25, 2020; revision requested September 21 and received November 18; accepted December 14. For this journal-based SA-CME activity, the author P.P.A. has provided disclosures (see end of article); all other authors, the editor, and the reviewers have disclosed no relevant relationships. **Address correspondence to** E.M.L. (e-mail: *echaripa@med.umich.edu*).

SA-CME LEARNING OBJECTIVES

After completing this journal-based SA-CME activity, participants will be able to:

- Describe the types of MRI artifacts caused by metal devices.
- Discuss how to change MRI parameters and patient factors to reduce metal artifact.
- List advanced imaging techniques that can be used in the setting of metal implants.

See rsna.org/learning-center-rg.

Introduction

The number of implanted devices continues to rise, and many patients with implanted devices may develop or have clinical conditions that are best depicted at MRI. It is estimated that the number of implanted devices will continue to rise because of changing demographics, device innovation, and an increase in the clinical indications for which devices are recommended. A world survey of cardiac implantable electronic devices (CIEDs) reported over 700 000 devices placed in 2009, and this number is likely to be an underestimation because of data missing from some countries (1). The American Academy of Orthopaedic Surgeons American Joint

TEACHING POINTS

- Implanted devices can cause a variety of artifacts at MRI, including signal loss, signal pileup, image distortion, failure of fat suppression, and ineffective signal nulling.
- Before scheduling a patient for an MRI examination, knowledge of the presence of an implant and location to undergo imaging is paramount.
- Similar to decreasing section thickness, increasing the image matrix results in smaller voxels that in turn decrease intravoxel signal loss.
- Fat-saturation techniques that rely on the frequency difference between fat and water assume a homogeneous resonance frequency of protons located within fat . The resonance frequency of protons near metal implants is altered, and therefore perfect fat saturation is not achieved because of the mismatch between the expected frequency and actual frequency.
- Like SEMAC, MAVRIC sequences require longer imaging times and have an increased SAR, which are primary drawbacks.

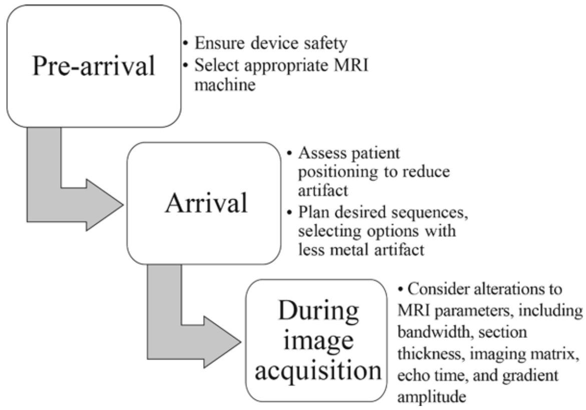

Figure 1. Flowchart shows the general approach to performing imaging in a patient with a metal implant. At multiple steps in the imaging process, decisions should be made to improve imaging quality and safety in those with metal implants.

Replacement Registry recorded 427 000 hip or knee replacements or replacement revisions in 2016, which is also likely to be an underestimation of the number of procedures actually performed since all institutions and surgeons in the United States are not required to submit to this registry (2).

As the number of implants has increased, so have the indications for which MRI is the preferred imaging modality. Hence, development of metal-suppression sequences has been an area of interest for various radiologic subspecialties. Radiologists now have access to advanced techniques for reducing metal artifact at MRI, and understanding and appropriately changing MRI parameters of standard sequences can help reduce artifact. Additional factors such as patient positioning, magnet strength, and availability of advanced imaging techniques (for example, specialized sequences that may only be available in specific MRI systems) must also be considered.

When planning to perform imaging in a patient with an implant, the following questions should be reviewed to optimize imaging quality (Fig 1): *(a)* Is there a specific MRI machine that is preferred for this patient? *(b)* If the implant is not directly undergoing imaging, is there a way to increase the distance of the implant from the imaging planes or change the orientation of the implant relative to the magnetic field to reduce artifact? *(c)* What specific sequences should be considered to minimize artifact? *(d)* How can MRI parameters be modified to minimize artifact?

We describe why MRI artifacts occur in the setting of implants. Strategies to reduce artifact as well as advanced imaging sequences for metal reduction are discussed.

Artifacts Related to Implanted Devices

Implanted devices can cause a variety of artifacts at MRI, including signal loss, signal pileup, image distortion, failure of fat suppression, and ineffective signal nulling. These artifacts are caused by a difference in magnetic susceptibility between the implant and adjacent soft tissues. The magnetic susceptibility of a substance describes how magnetized it becomes within a given magnetic field (Fig 2). Diamagnetic substances (eg, water) have negative susceptibility, which means that the internal magnetic field of water is reduced compared with the external magnetic field. Most biologic tissues are weakly diamagnetic. Paramagnetic and ferromagnetic substances have positive susceptibility; that is, these materials concentrate the magnetic field. This alters magnetization in the surrounding tissues and makes it less homogeneous.

The alteration to the local magnetic field is greater when implants contain ferromagnetic (eg, cobalt, iron, and nickel) rather than paramagnetic (eg, gadolinium) substances. In addition to their strong susceptibility, ferromagnetic materials have a magnetic memory and remain positively magnetized even after they have been removed from a magnetic field, thereby causing the most severe artifacts.

Fortunately, many newer implants, such as those used in musculoskeletal disorders, are made of titanium and other paramagnetic substances that cause less perturbation to the local magnetic field and therefore less artifact. There are continuous advances in this field that are aimed at improving MRI in the setting of implants with the development of novel materials, for example, carbon-fiber–reinforced polymers, which have been shown to have even further reduction in MRI artifacts as compared with titanium (3).

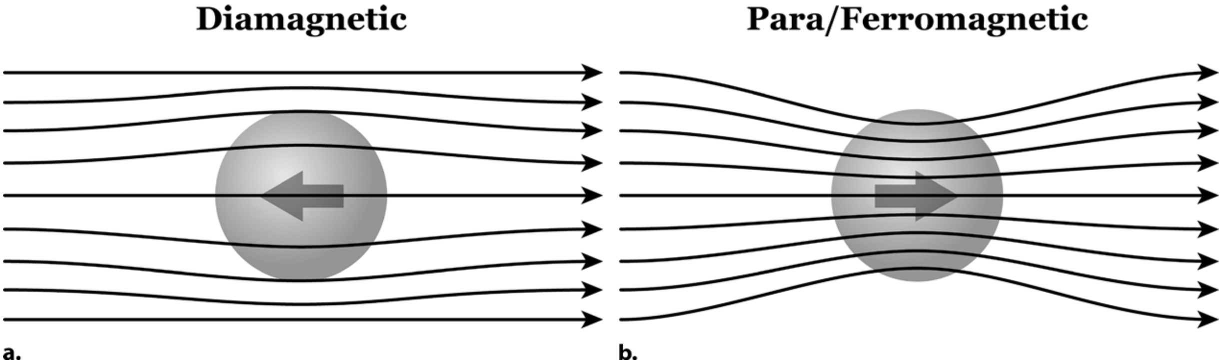

Figure 2. Drawings depict magnetic susceptibility, which describes how a material behaves when placed in a magnetic field. **(a)** A diamagnetic substance has negative susceptibility, as its internal magnetic field decreases when located in an external magnetic field. **(b)** Paramagnetic and ferromagnetic substances have positive susceptibility.

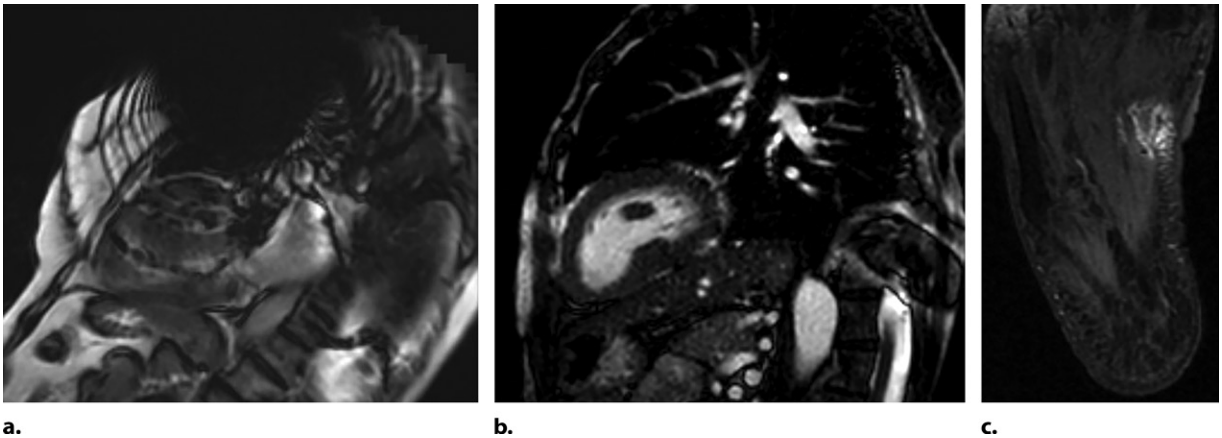

Figure 3. Spectrum of MRI artifacts from metal implants. **(a)** Cardiac localizer MR image in a patient with a cardiac implantable electronic device (CIED) shows a large area of signal loss and pileup from an implant. **(b)** Two-chamber steady-state free-precession (SSFP) MR image in a patient with an implant shows an artifact over the spine caused by image distortion from the implant. **(c)** Axial T1-weighted fat-saturated MR image of the plantar aspect of the foot shows how embedded metal prevents homogeneous fat suppression.

Signal Loss and Signal Pileup

Changes in the local magnetic field affect both the phase and frequency of the nearby protons. When the proton phase is perturbed, signal loss occurs (Fig 3). Within a given voxel, dephasing occurs quickly because of the inhomogeneity of the magnetic field locally, also known as the T2* effect. Additionally, the resonance of protons may be altered so that it is outside the frequency of the bandwidth of the radiofrequency pulse (4). In fact, this spatially shifted signal could lead to both signal loss (absence of signal from expected location) or signal pileup (increased signal at a certain location). Furthermore, the prosthesis itself contributes to lack of signal and signal void.

A four-leaf clover or dipole pattern can be seen at imaging, corresponding to a spherical ferromagnetic body that becomes magnetized and acts as a dipole aligned to the magnetic field (Fig 4). The interaction of the field lines of the dipole and the outside magnetic field lead to inhomogeneity with suppression as well as enhancement of the local field (B0), producing a four-leaf clover pattern characterized by curvilinear bands of signal loss and signal pileup (5,6).

Image Distortion

Image distortion is the result of misregistration of spatial information and occurs mostly in the frequency and section selection directions. Again, the local fields created by the ferromagnetic or paramagnetic implant alter surrounding tissue magnetization. Since MRI relies on linearity of the gradient fields for signal localization, when this linearity is altered, spatial localization is misregistered during readout, leading to in-plane and through-plane distortion (Fig 5) (7).

Failure of Fat Suppression

Techniques for fat suppression that rely on homogeneous resonance of protons within a given tissue are more susceptible to artifact in the presence of an implant compared with other sequences. In the setting of an implant, the

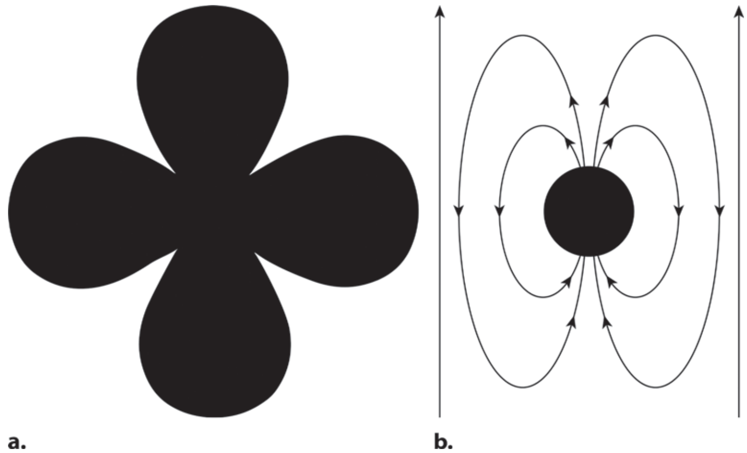

Figure 4. Drawings show how spherical ferromagnetic material acts as a dipole aligned to the magnetic field and leads to inhomogeneity of suppression, as well as enhancement of the local field (B0). This results in a four-leaf clover pattern.

resonance of nearby protons becomes heterogeneous. Therefore, a frequency-based saturation pulse such as spectral presaturation with inversion recovery (SPIR) may not have the desired effect and would fail to suppress fat protons not resonating at the expected frequency. Furthermore, water protons may start to resonate at a different frequency, approaching that of fat, and may become inadvertently suppressed, resulting in erroneous signal loss. It should be noted that T1-based fat-suppression techniques (eg, short τ inversion recovery [STIR]) are more effective in the presence of metal, as these techniques are based on the difference in T1 longitudinal relaxation between fat and water rather than the difference in resonance frequency between fat and water, as in frequency-based fat-saturation techniques such as SPIR.

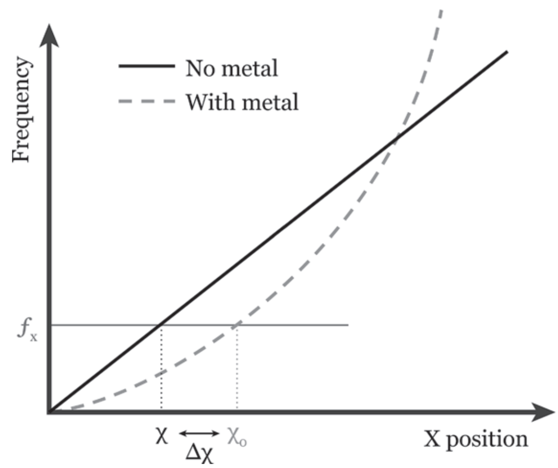

Figure 5. Graph shows how misregistration of spatial information occurs, as MRI relies on linearity of the gradient field (black solid line) for localization, but this linearity is altered in the presence of metal implants (gray dashed line). This leads to a change in spatial location (Δχ), leading to in-plane and through-plane distortions. f_x = frequency, X = position.

Strategies to Decrease Metal Artifact on MR Images

The following categories can be addressed to improve MR images in the presence of a metal implant: MRI parameters, patient position, and MRI sequences (Table).

MRI Parameters

Field Strength.—Before scheduling a patient for an MRI examination, knowledge of the presence of an implant and location to undergo imaging is paramount. Lower field-strength imaging may be preferred to mitigate metal-related artifact. The relationship between artifact and magnetic field strength is linear, that is, examinations performed with a 1.5-T magnet would have half the artifact compared with those performed with a 3-T magnet. However, a lower field strength also decreases signal-to-noise ratio (SNR). In some cases, artifact size at 3 T can be reduced by adjusting MRI parameters to an acceptable level, so imaging may still be better at 3 T relative to 1.5 T (8, 9).

Increase Bandwidth.—Readout bandwidth is the range of frequencies sampled or received by the imaging system. As metal implants lead to an increase in the variance of frequencies, if the bandwidth is increased, there will be a better overlap between the frequencies sampled and the actual frequencies present. Since bandwidth depends on a combination of field of view (FOV) and frequency-encoding gradient strength, for a given FOV, increasing the gradient increases the maximum resonant frequency and thereby the range of frequencies (ie, bandwidth).

The sampling frequency is typically at least twice the maximum resonant frequency and is inversely related to the sampling interval. With an increase in sampling frequency, there is a corresponding decrease in the sampling time (proportional to 1/bandwidth), which decreases the impact of the variance in frequencies on spatial encoding. Typically, bandwidth should be doubled or tripled. This also has the advantage of reduced

Adjustments to Reduce Metal Artifact

Parameter	Adjustment	Effect	Comments
Field strength	Decrease	Higher field strengths result in more local magnetic field heterogeneity	Lower field strength decreases SNR Altering other MRI parameters may allow acceptable imaging quality at 3 T
Bandwidth	Increase (double or triple)	Reduces sampling time, which decreases the impact of variance in frequencies on spatial encoding	Decreases SNR
Section thickness	Decrease	Decreases voxel size, limiting voxels affected by artifact	Decreases SNR
Matrix	Increase	Decreases voxel size, limiting voxels affected by artifact	Decreases SNR Most effective when done in the frequency-encoding direction
TE	Decrease	Decreases variation in spin dephasing	NA
Gradient amplitude	Increase	Increase the frequencies encoded in each voxel so any change in frequency has less effect on spatial encoding Also decreases TE (leading to less time for dephasing)	Decreases SNR
Patient positioning	If possible, distance the device as far as possible from the desired site to be imaged Align the long axis of the implant with the B0 Align the frequency-encoding gradient to the long axis of the implant	Metal artifacts decrease with increasing distance, as they reflect alteration to the local magnetic field	Positioning maneuvers may not always be possible Aligning the frequency gradient increases imaging time
MRI sequence	FSE (instead of GRE)	Shorter TR decreases metal artifact	Image blurring with FSE
	STIR or Dixon (instead of sequences relying on spectral frequencies for nulling)	By not relying on spectral frequencies (which are altered in the presence of metal), better nulling of signal can occur	NA
	Fast spoiled gradient echo (instead of SSFP imaging)	Short TR decreases metal artifact	NA
	Specialized sequences (wideband in cardiac MRI for cardiac imaging or metal reduction [MARS])	NA	MARS has a higher SAR and longer imaging time

Note.—FSE= fast spin echo, GRE = gradient echo, MARS = metal artifact reduction sequence, NA = not available, SAR = specific absorption rate, SNR = signal-to-noise ratio, STIR = short τ inversion recovery, TE = echo time, TR = repetition time.

echo spacing (mentioned later in the article) and reduced acquisition time. As a consequence, the SNR is reduced and may need to be compensated by increasing the number of signal averages. Overall, the effect of increased bandwidth and increased signal averages would lead to longer imaging time.

Decrease Section Thickness.—By decreasing section thickness, voxel size is reduced. This decreases the voxels that are affected by dephasing and ultimately decreases metal artifact. However, decreasing section thickness comes at the cost of decreased SNR.

Increase Image Matrix.—Similar to decreasing section thickness, increasing the image matrix results in smaller voxels that in turn decrease intravoxel signal loss. This is also at the cost of decreased SNR. Increasing the imaging matrix is most effective when done in the frequency-encoding direction, as increasing the matrix in the phase-encoding direction results in a longer imaging time.

Reduce Echo Time.—Reducing echo time (TE) minimizes variations in dephasing, thereby reducing metal artifact. To review, TE is the duration of time between an excitation pulse and signal data acquisition. After an excitation pulse, transverse magnetization is lost over time because of T2* relaxation, which is the combined effect of intrinsic T2 decay (not recoverable) and spins dephasing, with the latter increasing in the presence of metal implants. Shortly after an excitation pulse, transverse magnetization is composed of in-phase spins. Over time, the magnetic field distortion caused by the metal implant causes spins to go out of phase, and therefore the transverse magnetization (composed of the spins' vector sum) is reduced and metal artifact becomes more pronounced. By using a short TE, the amount of spin dephasing is reduced, and thus metal artifact is decreased (Fig 6).

Switch to Nonselective or Wideband Radiofrequency Pulses.—An inversion-recovery approach is used in certain applications when signal nulling is required such as in late gadolinium enhancement (LGE) assessment at cardiac MRI. In this case, a section-selective inversion pulse may not effectively result in magnetization inversion and signal nulling because of frequency offset in the presence of metal. Switching to nonselective or wideband radiofrequency pulses resolves this issue, as explained in the pulse sequences section.

Patient Position

Alignment of Device with B0.—Artifact from metal implants is smallest when the long axis of the implant is aligned with the main magnetic field (B0) direction. In some cases (eg, orthopedic implants), the body can be positioned to allow the long axis to align with B0 (10). In many cases, patient repositioning to allow alignment is not possible given the location of the device, region to be imaged, and architecture of MRI machines. This is true for most intra-abdominal, intracranial, and intrathoracic implants.

When the position of the implant cannot be changed, the frequency-encoding gradient can be aligned parallel to the long axis of the implant. This minimizes metal artifact but increases imaging time. In some cases, such as for round metal implants that inherently cause more artifact, changing the frequency-encoding gradient is not possible given the lack of a long axis.

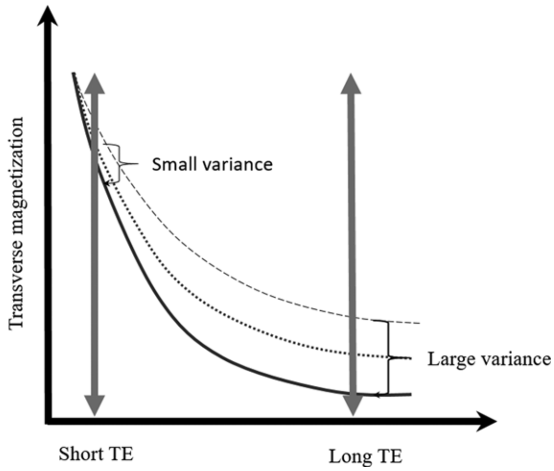

Figure 6. Graph demonstrates the relationship of TE and transverse magnetization. Over time, transverse magnetization decreases, and the degree of loss of transverse magnetization is greater near metal implants. By utilizing a short TE, the differences between transverse magnetization are mitigated, therefore decreasing the artifacts.

Movement of Device Away from Desired Anatomy.—In some occasions, the body may be repositioned or respiratory maneuvers may be performed that allow a greater distance between the desired area of imaging and the location of the implant, thereby decreasing artifact in the imaged anatomy. For example, a CIED may move farther away from the heart when the extremity ipsilateral to the implant is raised (Fig 7). Additional respiratory maneuvers (ie, performing imaging during end inspiration when the diaphragm has flattened and the cardiac structures have moved more inferiorly and away from a chest implant) may also be helpful in certain circumstances.

MRI Sequences

Fast Spin Echo.—Fast spin echo (FSE) uses 180° refocusing pulses to reduce dephasing (in contrast to gradient-echo sequences) and allows multiple lines of k-space to be acquired within a given repetition time (TR), in contrast to conventional spin echo. Gradient-echo sequences do not use refocusing pulses and are therefore markedly susceptible to field inhomogeneities (Fig 8). While it is not always possible to replace gradient-echo sequences with FSE sequences, care should be taken to strategically select the most appropriate sequence to answer the specific clinical question. However, FSE images may have some blurring owing to the long TE and TR times, secondary to the nature of the FSE sequence structure (90° and 180° acquisition), compared with images obtained with gradient-echo sequences, which use small flip

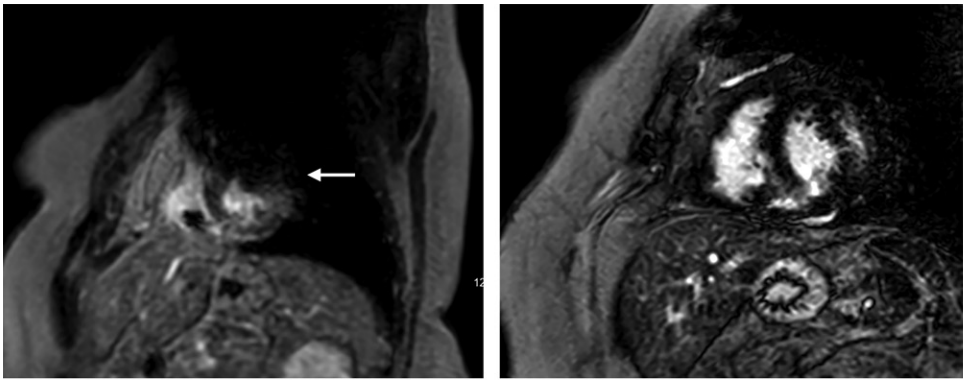

a. b.

Figure 7. Impact of patient positioning on metal artifact. **(a)** Short-axis late gadolinium enhancement (LGE) MR image obtained in a patient positioned with arms by their sides shows an artifact (arrow) from a CIED obscuring the anterior wall of the left ventricle. **(b)** Short-axis LGE MR image shows how the artifact is nearly resolved when the patient's arms are raised, which moves the CIED generator farther from the imaging area of interest. Patient positioning can be optimized to reduce metal artifact depending on the device and anatomic location to be imaged.

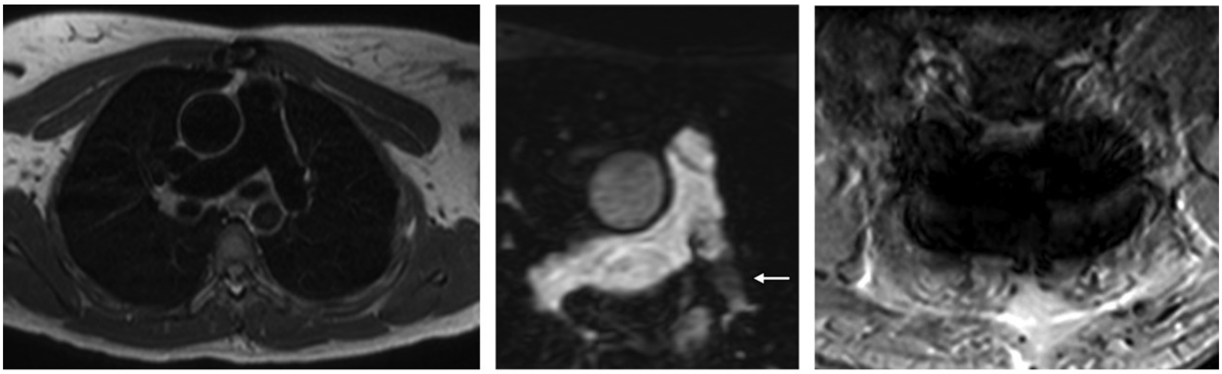

a. b. c.

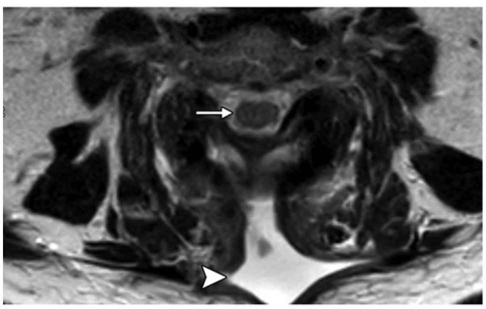

d.

Figure 8. FSE uses multiple refocusing pulses and thereby reduces metal artifact by decreasing T2* effects. **(a)** Axial proton-density–weighted dark-blood FSE MR image obtained in a patient with tetralogy of Fallot and a left pulmonary artery stent shows a reduced artifact through the left pulmonary artery. **(b)** Axial gadolinium-enhanced MR angiogram, for which the series of refocusing pulses were not used, shows the artifact more clearly (arrow). **(c)** Axial T2-weighted GRE MR image of the lower cervical spine obtained in a patient with a history of posterior instrumentation and fusion shows significant susceptibility artifact due to the hardware that is present. **(d)** Axial T2-weighted FSE MR image shows how the artifact in **c** has been mitigated. The spinal canal (arrow) and posterior subcutaneous fluid collection (arrowhead) are better appreciated on this image.

angles without 180° refocusing pulses. Furthermore, FSE does not help with spatial misregistration that can occur in the setting of implants (11).

STIR and Dixon.—Fat-saturation techniques that rely on the frequency difference between fat and water assume a homogeneous resonance frequency of protons located within fat (12). The resonance frequency of protons near metal implants is altered, and therefore perfect fat saturation is not achieved because of the mismatch between the expected frequency and actual frequency. Not only may areas of fat not saturate, but nonfat tissue may saturate if its frequency happens to be altered by the adjacent metal and matches the expected frequency of fat.

Since the STIR technique is not based on the frequency difference between fat and water, it is unaffected by metal-induced frequency shifts (Fig 9). In comparison with spectral-based fat-saturation techniques, STIR is based on the different T1 values of fat and water. Fat-suppression effectiveness by using STIR can be maximized by matching the bandwidth of the inversion pulse to the excitation pulse. When not matched, the excitation section may not be inverted, and the

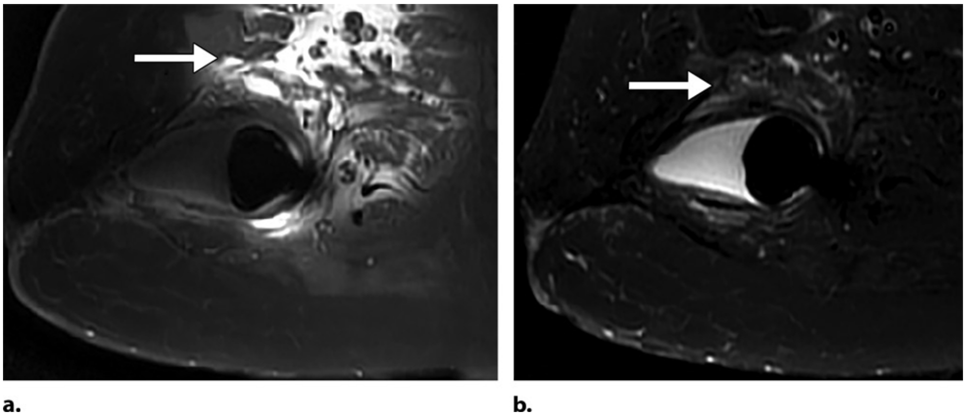

Figure 9. Spectral presaturation with inversion recovery (SPIR) relies on spectral frequencies to null fat. (a) Axial SPIR MR image in a patient with a history of hip arthroplasty shows significant artifacts (arrow), as the metal has altered the expected frequencies of protons near the implant. This leads to incomplete fat suppression. (b) Axial STIR MR image shows better fat suppression (arrow), as STIR relies on T1 relaxation.

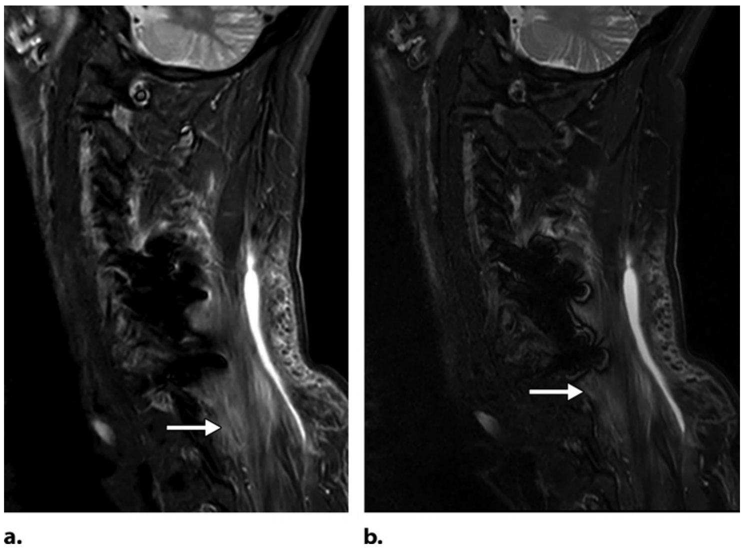

Figure 10. STIR and Dixon imaging. Sagittal T2-weighted STIR MR image (a) and sagittal Dixon T2-weighted fat-suppressed MR image (b) obtained near the midline in a patient with posterior cervical spine instrumentation show improved fat suppression in the Dixon T2-weighted MR image (arrow in b) compared with the T2-weighted STIR image (arrow in a). These images illustrate the challenge of achieving high-quality fat suppression with metallic instrumentation even with STIR or Dixon imaging, but there is a slight advantage of using Dixon imaging in this setting.

inversion may be displaced to other sections in the presence of metal (13).

Dixon imaging relies on differentiation of the chemical shift of water and fat to create images. The Dixon technique has a better SNR compared with STIR and has the added benefit of reliably obtaining both water and fat images in one acquisition (Fig 10) (14). Compared with STIR, it is more affected by metal artifacts.

Fast Gradient Echo.—The use of a fast spoiled gradient-echo sequence instead of steady-state free-precession (SSFP) imaging, which is commonly used for ventricular size and function assessment in cardiac imaging, can result in decreased metal artifact at the cost of lower SNR. SSFP imaging requires a longer TR, thereby leading to more artifact compared with a fast gradient-echo sequence (Fig 11). Artifact can be further reduced by decreasing TE through partial Fourier readout and increasing the bandwidth, and thus reducing TR accordingly. However, this leads to lower SNR and resolution (15).

Advanced Sequences

Modified Wideband Inversion Recovery.—LGE cardiac MRI is the standard in identifying myocardial scar and arrhythmogenic substrates for potential targets for radiofrequency catheter ablation, a therapeutic modality that can eliminate arrhythmia and improve survival (16–22). Many of these patients have CIEDs, which present several challenges related to imaging, including safety and metal device–induced artifacts.

While potential device or lead malfunction were initially concerns regarding cardiac MRI in patients with CIEDs, many studies have shown that cardiac MRI can be safely performed in these patients (23–26). The diagnostic quality of cardiac MRI in patients with CIEDs has historically been limited because of metal device–induced signal

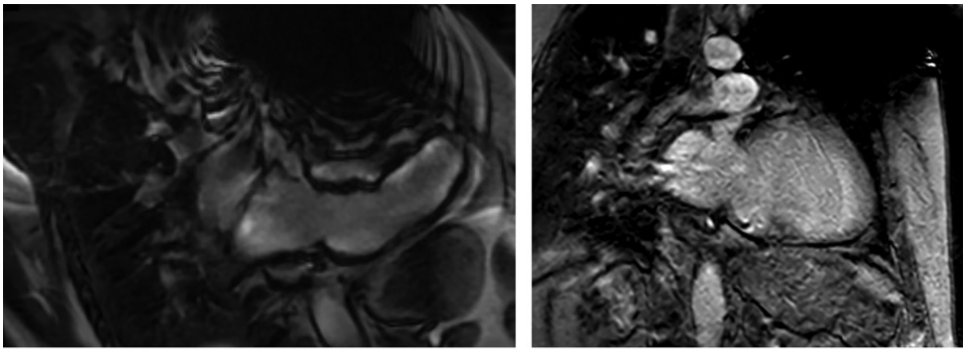

a. b.

Figure 11. SSFP imaging requires a uniform magnetic field and may show significant artifacts in the presence of a CIED. **(a)** Two-chamber SSFP MR image of the left ventricle shows artifact. **(b)** Two-chamber fast gradient-echo MR image shows less artifact, as the TR is shorter. Fast gradient-echo imaging can be used as an alternative. However, this comes at the price of a reduced SNR.

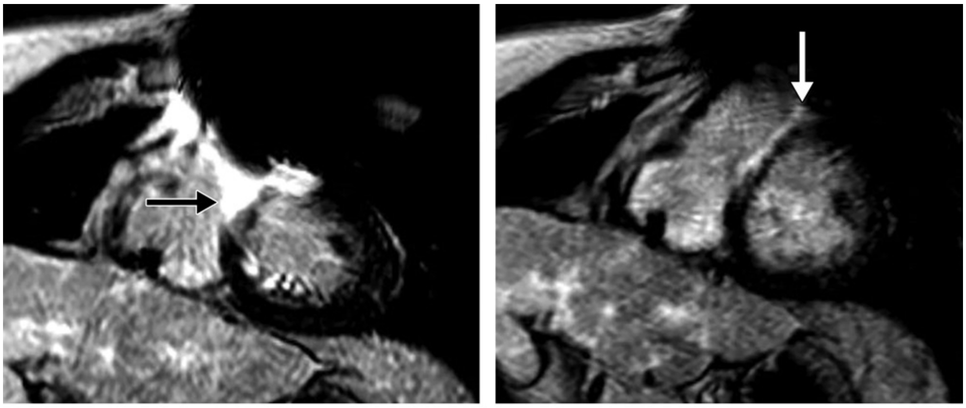

a. b.

Figure 12. Metal device–induced hyperintensity artifact. **(a)** Short-axis conventional inversion-recovery MR image obtained in the presence of a CIED shows a hyperintense metal-induced artifact (arrow) obscuring the anterior and anteroseptal left ventricle. **(b)** Short-axis LGE MR image obtained with a wideband technique in the myocardium shows improved image quality (arrow).

nulling and hyperintensity artifacts that obscure the anatomic region of interest (27–31) (Fig 12). The hyperintense artifact is due to the off resonance of the myocardium near the CIED. This myocardium does not have the same inversion time as other sections of the myocardium farther away from the implant and therefore does not null as expected, leading to a hyperintense artifact.

In recent years, a novel modified wideband inversion-recovery technique has been used to successfully decrease the severity of device-related artifacts while maintaining anatomic detail and diagnostic image quality (32–36). This novel technique utilizes an inversion-recovery radiofrequency pulse with wider frequency bandwidth, which makes it effective even with frequency shift caused by the metal implant (Fig 13). This alleviates hyperintensity artifacts that obscure anatomy and can mimic scars.

Metal Artifact Reduction Sequences.—Some specific commonly used metal artifact reduction sequences (MARSs) include slice encoding for metal artifact correction (SEMAC) and multiacquisition with variable-resonance image combination (MAVRIC) (Fig 14) (37). SEMAC is a multispectral two-dimensional FSE or turbo spin-echo technique that reduces through-plane distortion. Each imaged section in a SEMAC sequence is phase encoded in the third dimension, which is called z-phase encoding. This information from all the overlapping sections provides a detailed map of exactly how magnetic susceptibility has distorted the image. SEMAC is used in combination with view angle tilting, a technique that adds a compensatory section-selection gradient with the conventional readout gradient, which ultimately results in all off-resonance–induced shifts along the readout direction being "sheared" away (5). SEMAC sequences, because of their use of three-dimensional (3D) encoding of each section, require longer imaging times, which is the major drawback to their use. SEMAC has been shown to be superior to

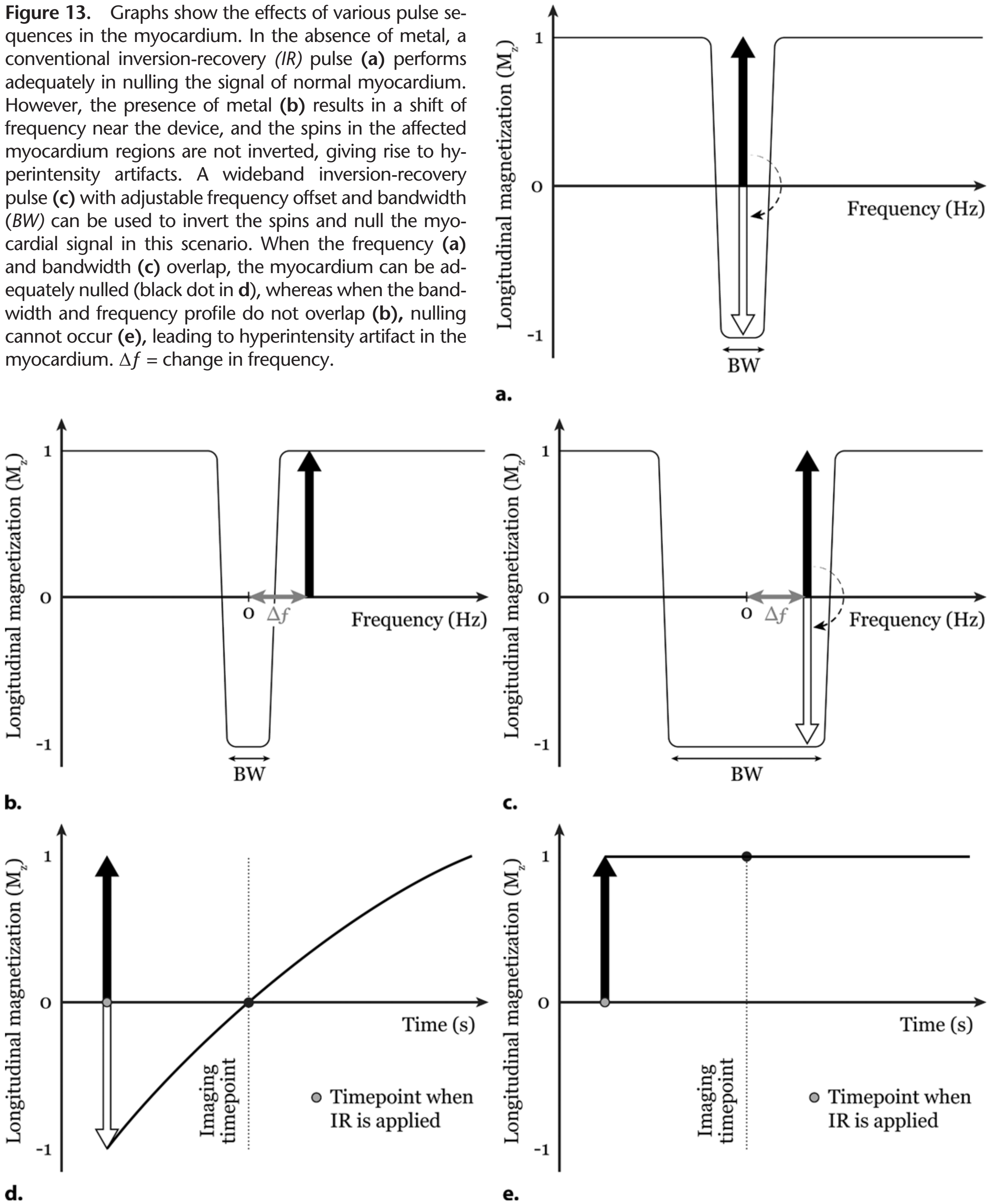

Figure 13. Graphs show the effects of various pulse sequences in the myocardium. In the absence of metal, a conventional inversion-recovery *(IR)* pulse **(a)** performs adequately in nulling the signal of normal myocardium. However, the presence of metal **(b)** results in a shift of frequency near the device, and the spins in the affected myocardium regions are not inverted, giving rise to hyperintensity artifacts. A wideband inversion-recovery pulse **(c)** with adjustable frequency offset and bandwidth (*BW)* can be used to invert the spins and null the myocardial signal in this scenario. When the frequency **(a)** and bandwidth **(c)** overlap, the myocardium can be adequately nulled (black dot in **d**), whereas when the bandwidth and frequency profile do not overlap **(b),** nulling cannot occur **(e),** leading to hyperintensity artifact in the myocardium. Δf = change in frequency.

standard MRI sequences and high-bandwidth protocols that do not use MARS (38–40).

MAVRIC is a multispectral spatially nonselective spin-echo–based 3D acquisition technique that addresses both through-plane and in-plane artifacts. It uses multidirectional VAT to minimize in-plane distortions by adding an altered readout gradient, a series of frequency-selective excitations, and computational postprocessing. MAVRIC uses a standard 3D readout, in which it utilizes proprietary smoothing and antiblurring algorithms to further increase diagnostic quality of images. Like SEMAC, MAVRIC sequences require longer imaging times and have an increased specific absorption rate (SAR), which are primary drawbacks. The reason for an increased SAR in MAVRIC is the high-bandwidth and 3D FSE acquisition, which are needed to suppress metal artifacts. Furthermore, both MAVRIC and SEMAC acquire a large number of signal acquisitions, which also increases SAR. Although the SAR limit may not be reached at low-field (up to 1.5-T) imaging, this may not be the case at a higher magnetic field, where SAR calculations could exceed the allowed limit, resulting in automatic adjustment of other sequence parameters and therefore a suboptimal imaging condition (41).

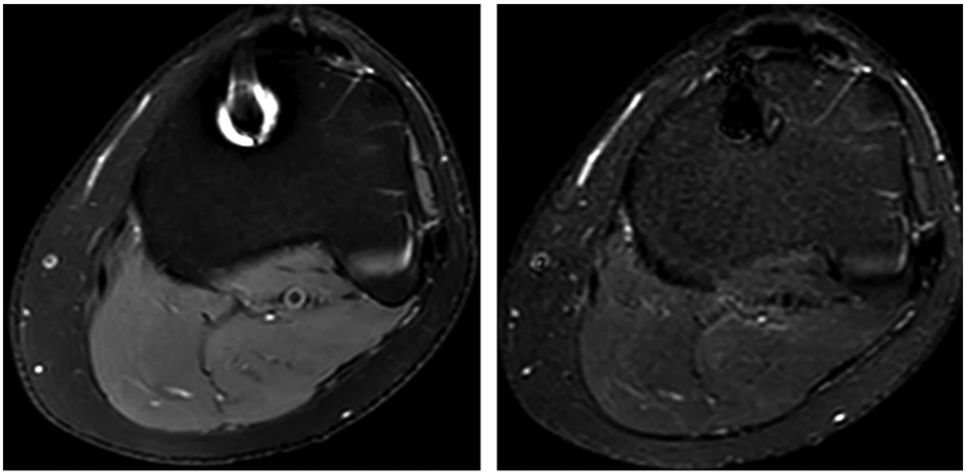

a. b.

Figure 14. Metal artifact reduction sequence (MARS) in a patient with a history of anterior cruciate ligament repair. **(a)** Axial STIR MR image of the knee obtained without MARS shows artifact. **(b)** Axial STIR MR image obtained with MARS shows artifact reduction.

Furthermore, another potential disadvantage of MAVRIC, particularly when imaging the hip or shoulder joint, is aliasing in the through-plane direction due to the spatially nonselective 3D volume excitation (42). Even more advanced techniques such as MAVRIC-SEMAC hybrids and off-resonance suppression techniques are not yet in widespread clinical practice but have been developed.

Conclusion

MRI is commonly requested in patients with metal implants. Multiple methods for decreasing artifacts can be used to improve image quality and increase diagnostic confidence. Performing imaging in these patients requires careful consideration of the type and location of metal implant, locally available scanners and sequences, the clinical question, and knowledge of MRI parameters and their impact on artifact.

Acknowledgment.—The authors thank Danielle Dobbs for providing the images in Figures 2, 4, 5, and 13.

Disclosures of Conflicts of Interest.—**P.P.A.** *Activities related to the present article:* disclosed no relevant relationships. *Activities not related to the present article:* institution received grants from SPIROMICS II and MyoKardia. *Other activities:* disclosed no relevant relationships.

References

1. Mond HG, Proclemer A. The 11th world survey of cardiac pacing and implantable cardioverter-defibrillators: calendar year 2009—a World Society of Arrhythmia's project. Pacing Clin Electrophysiol 2011;34(8):1013–1027.
2. American Joint Replacement Registry, American Academy of Orthopaedic Surgeons. 2016 Report to the Public About Hip and Knee Replacements. https://www.aaos.org/globalassets/registries/ajrr_patient_summary_2016_ar_final.pdf. Published April 13, 2020. Accessed October 18, 2019.
3. Zimel MN, Hwang S, Riedel ER, Healey JH. Carbon fiber intramedullary nails reduce artifact in postoperative advanced imaging. Skeletal Radiol 2015;44(9):1317–1325.
4. Khodarahmi I, Isaac A, Fishman EK, Dalili D, Fritz J. Metal About the Hip and Artifact Reduction Techniques: From Basic Concepts to Advanced Imaging. Semin Musculoskelet Radiol 2019;23(3):e68–e81.
5. Jungmann PM, Agten CA, Pfirrmann CW, Sutter R. Advances in MRI around metal. J Magn Reson Imaging 2017;46(4):972–991.
6. Aboelmagd SM, Malcolm PN, Toms AP. Magnetic resonance imaging of metal artifact reduction sequences in the assessment of metal-on-metal hip prostheses. Rep Med Imaging 2014;7:65–74.
7. Khodarahmi I, Fishman EK, Fritz J. Dedicated CT and MRI Techniques for the Evaluation of the Postoperative Knee. Semin Musculoskelet Radiol 2018;22(4):444–456.
8. Olsrud J, Lätt J, Brockstedt S, Romner B, Björkman-Burtscher IM. Magnetic resonance imaging artifacts caused by aneurysm clips and shunt valves: dependence on field strength (1.5 and 3 T) and imaging parameters. J Magn Reson Imaging 2005;22(3):433–437.
9. Fritz J, Lurie B, Miller TT, Potter HG. MR imaging of hip arthroplasty implants. RadioGraphics 2014;34(4):E106–E132.
10. Harris CA, White LM. Metal artifact reduction in musculoskeletal magnetic resonance imaging. Orthop Clin North Am 2006;37(3):349–359, vi.
11. Gupta A, Subhas N, Primak AN, Nittka M, Liu K. Metal artifact reduction: standard and advanced magnetic resonance and computed tomography techniques. Radiol Clin North Am 2015;53(3):531–547.
12. Delfaut EM, Beltran J, Johnson G, Rousseau J, Marchandise X, Cotten A. Fat suppression in MR imaging: techniques and pitfalls. RadioGraphics 1999;19(2):373–382.
13. Ulbrich EJ, Sutter R, Aguiar RF, Nittka M, Pfirrmann CW. STIR sequence with increased receiver bandwidth of the inversion pulse for reduction of metallic artifacts. AJR Am J Roentgenol 2012;199(6):W735–W742.
14. Ma J. Dixon techniques for water and fat imaging. J Magn Reson Imaging 2008;28(3):543–558.
15. Olivieri LJ, Cross RR, O'Brien KE, Ratnayaka K, Hansen MS. Optimized protocols for cardiac magnetic resonance imaging in patients with thoracic metallic implants. Pediatr Radiol 2015;45(10):1455–1464.
16. Kwong RY, Korlakunta H. Diagnostic and prognostic value of cardiac magnetic resonance imaging in assessing myocardial viability. Top Magn Reson Imaging 2008;19(1):15–24.
17. Hombach V, Merkle N, Bernhard P, Rasche V, Rottbauer W. Prognostic significance of cardiac magnetic resonance imaging: Update 2010. Cardiol J 2010;17(6):549–557.
18. Kim HW, Farzaneh-Far A, Kim RJ. Cardiovascular magnetic resonance in patients with myocardial infarction: current and emerging applications. J Am Coll Cardiol 2009;55(1):1–16.
19. Wu HD, Kwong RY. Cardiac magnetic resonance imaging in patients with coronary disease. Curr Treat Options Cardiovasc Med 2008;10(1):83–92.
20. Kuck KH, Schaumann A, Eckardt L, et al. Catheter ablation of stable ventricular tachycardia before defibrillator implantation in patients with coronary heart disease

(VTACH): a multicentre randomised controlled trial. Lancet 2010;375(9708):31–40.
21. Yokokawa M, Kim HM, Baser K, et al. Predictive value of programmed ventricular stimulation after catheter ablation of post-infarction ventricular tachycardia. J Am Coll Cardiol 2015;65(18):1954–1959.
22. Reddy VY, Reynolds MR, Neuzil P, et al. Prophylactic catheter ablation for the prevention of defibrillator therapy. N Engl J Med 2007;357(26):2657–2665.
23. Nazarian S, Hansford R, Roguin A, et al. A prospective evaluation of a protocol for magnetic resonance imaging of patients with implanted cardiac devices. Ann Intern Med 2011;155(7):415–424.
24. Nazarian S, Roguin A, Zviman MM, et al. Clinical utility and safety of a protocol for noncardiac and cardiac magnetic resonance imaging of patients with permanent pacemakers and implantable-cardioverter defibrillators at 1.5 tesla. Circulation 2006;114(12):1277–1284.
25. Horwood L, Attili A, Luba F, et al. Magnetic resonance imaging in patients with cardiac implanted electronic devices: focus on contraindications to magnetic resonance imaging protocols. Europace 2017;19(5):812–817.
26. Russo RJ, Costa HS, Silva PD, et al. Assessing the Risks Associated with MRI in Patients with a Pacemaker or Defibrillator. N Engl J Med 2017;376(8):755–764.
27. Mesubi O, Ahmad G, Jeudy J, et al. Impact of ICD artifact burden on late gadolinium enhancement cardiac MR imaging in patients undergoing ventricular tachycardia ablation. Pacing Clin Electrophysiol 2014;37(10):1274–1283.
28. Ibrahim EH, Runge M, Stojanovska J, et al. Optimized cardiac magnetic resonance imaging inversion recovery sequence for metal artifact reduction and accurate myocardial scar assessment in patients with cardiac implantable electronic devices. World J Radiol 2018;10(9):100–107.
29. Buendía F, Cano Ó, Sánchez-Gómez JM, et al. Cardiac magnetic resonance imaging at 1.5 T in patients with cardiac rhythm devices. Europace 2011;13(4):533–538.
30. Dandamudi S, Collins JD, Carr JC, et al. The Safety of Cardiac and Thoracic Magnetic Resonance Imaging in Patients with Cardiac Implantable Electronic Devices. Acad Radiol 2016;23(12):1498–1505.
31. Sasaki T, Hansford R, Zviman MM, et al. Quantitative assessment of artifacts on cardiac magnetic resonance imaging of patients with pacemakers and implantable cardioverter-defibrillators. Circ Cardiovasc Imaging 2011;4(6):662–670.
32. Runge M, Ibrahim EH, Bogun F, et al. Metal Artifact Reduction in Cardiovascular MRI for Accurate Myocardial Scar Assessment in Patients With Cardiac Implantable Electronic Devices. AJR Am J Roentgenol 2019;213(3):555–561.
33. Singh A, Kawaji K, Goyal N, et al. Feasibility of Cardiac Magnetic Resonance Wideband Protocol in Patients With Implantable Cardioverter Defibrillators and Its Utility for Defining Scar. Am J Cardiol 2019;123(8):1329–1335.
34. Do DH, Eyvazian V, Bayoneta AJ, et al. Cardiac magnetic resonance imaging using wideband sequences in patients with nonconditional cardiac implanted electronic devices. Heart Rhythm 2018;15(2):218–225.
35. Hilbert S, Weber A, Nehrke K, et al. Artefact-free late gadolinium enhancement imaging in patients with implanted cardiac devices using a modified broadband sequence: current strategies and results from a real-world patient cohort. Europace 2018;20(5):801–807.
36. Stevens SM, Tung R, Rashid S, et al. Device artifact reduction for magnetic resonance imaging of patients with implantable cardioverter-defibrillators and ventricular tachycardia: late gadolinium enhancement correlation with electroanatomic mapping. Heart Rhythm 2014;11(2):289–298.
37. Talbot BS, Weinberg EP. MR Imaging with Metal-suppression Sequences for Evaluation of Total Joint Arthroplasty. RadioGraphics 2016;36(1):209–225.
38. Sutter R, Hodek R, Fucentese SF, Nittka M, Pfirrmann CW. Total knee arthroplasty MRI featuring slice-encoding for metal artifact correction: reduction of artifacts for STIR and proton density-weighted sequences. AJR Am J Roentgenol 2013;201(6):1315–1324.
39. Lee YH, Lim D, Kim E, Kim S, Song HT, Suh JS. Usefulness of slice encoding for metal artifact correction (SEMAC) for reducing metallic artifacts in 3-T MRI. Magn Reson Imaging 2013;31(5):703–706.
40. Sutter R, Ulbrich EJ, Jellus V, Nittka M, Pfirrmann CW. Reduction of metal artifacts in patients with total hip arthroplasty with slice-encoding metal artifact correction and view-angle tilting MR imaging. Radiology 2012;265(1):204–214.
41. Naganawa S, Kawai H, Fukatsu H, et al. High-speed imaging at 3 Tesla: a technical and clinical review with an emphasis on whole-brain 3D imaging. Magn Reson Med Sci 2004;3(4):177–187.
42. Takeuchi N, Mitsuyasu H, Nakanishi T, et al. The orientation of orthopaedic metallic devices relative to the frequency-encoding gradient affects susceptibility artifacts: an experiment using open MR imaging. Fukuoka Igaku Zasshi 2011;102(5):185–194.